

Efficient wind fragility analysis of RC high rise building through metamodelling

Apurva Bhandari^a, Gaurav Datta^b and Soumya Bhattacharjya^{*}

Department of Civil Engineering, Indian Institute of Engineering Science and Technology (IIST) Shibpur,
Howrah.-711103, West Bengal, India

(Received September 12, 2017, Revised April 24, 2018, Accepted May 2, 2018)

Abstract. This paper deals with wind fragility and risk analysis of high rise buildings subjected to stochastic wind load. Conventionally, such problems are dealt in full Monte Carlo Simulation framework, which requires extensive computational time. Thus, to make the procedure computationally efficient, application of metamodelling technique in fragility analysis is explored in the present study. Since, accuracy by the conventional Least Squares Method (LSM) based metamodelling is often challenged, an efficient Moving Least Squares Method based adaptive metamodelling technique is proposed for wind fragility analysis. In doing so, artificial time history of wind load is generated by three wind field models: i.e., a simple one based on alongwind component of wind speed; a more detailed one considering coherence and wind directionality effect, and a third one considering nonstationary effect of mean wind. The results show that the proposed approach is more accurate than the conventional LSM based metamodelling approach when compared to full simulation approach as reference. At the same time, the proposed approach drastically reduces computational time in comparison to the full simulation approach. The results by the three wind field models are compared. The importance of non-linear structural analysis in fragility evaluation has been also demonstrated.

Keywords: wind fragility; metamodelling; Moving Least Squares Method; risk; Monte Carlo Simulation; RC building

1. Introduction

High-rise buildings are the best solution to the scarce and expensive land acquirement in big cities and such buildings are becoming essential to the society. With time and advancement of technology, light weight superstructures are favored, from economy point of view, which in turn makes tall buildings more flexible and hence more vulnerable to naturally occurring wind loads. Thus, dynamic effect caused by wind has become an important consideration in safe design and occupants comfort in wind excited buildings. In order to assess prevailing risk of failure of tall buildings under stochastic wind effect, a fragility analysis must be performed. However, to assess fragility one must have i) realistic artificial generation of wind field, and ii) a computationally efficient and accurate wind fragility assessment procedure.

Conventionally, wind fragility analysis problems are dealt in full Monte Carlo Simulation (MCS) framework (Marra and Luca 2010, Gur and Chaudhuri 2014, Konthesingha *et al.* 2015). Most recently, Peng *et al.* (2018) presented wind fragility analysis of tree structure by the MCS. However, a major drawback of this approach is enormous computational time requirement for realistic complex engineering structures. Hence, this paper explores Response Surface Method (RSM) based metamodelling technique to partly replace the MCS in order to reduce

computational time in fragility analysis. In fact, owing to the advent of efficient sampling procedures in the RSM, relatively few structural analysis runs are required to build a reasonably accurate metamodel (Gupta and Manohar 2004). Generally, the RSM (Myers and Montgomery 1995) is based on the global approximation of scatter position data obtained by using the Least-Squares Method (LSM). However, the LSM is one of the major sources of error in prediction by the RSM (Bhattacharjya and Chakraborty 2011). In fact, the efficiency of RSM largely depends on the selection of the basis function and should be chosen to resemble the basis function as closely as possible to the actual variation of the response within the solution domain. The Moving Least-Squares Method (MLSM), which is a comparatively new approach of adaptive metamodelling, circumvent this problem of global approximation by establishing a local approximation around each point in the interpolation domain through varying weight functions with respect to the position of the approximation (Kim *et al.* 2005). Thus, in the present paper, the MLSM based adaptive RSM is explored to ensure accuracy by the metamodelling. The MLSM based RSM has been successfully used in reliability analysis (Kang *et al.* 2010, Lu *et al.* 2017) and optimization (Song *et al.* 2011). There have been studies addressing seismic reliability and stochastic optimization using the MLSM based RSM, as well (Bhattacharjya and Chakraborty 2011, Ghosh *et al.* 2016). Taflanidis *et al.* (2016) investigated hurricane response analysis and risk associated to land slide problem of Hawaiian island using the MLSM based metamodelling. However, study addressing wind fragility assessment of structure in the MLSM based RSM framework is observed to be scarce in existing literature. Hence, there is ample

*Corresponding author, Assistant Professor

E-mail: soumyaiiests@gmail.com

^a MTech. Scholar

^b Ph.D. Scholar

scope to explore fragility and risk analysis of wind excited structures in the MLSM based RSM framework which builds the scope of this study.

Estimation of realistic wind load is another important input for wind fragility analysis. According to the guidelines of most of the building Codes and Standards including Indian Standard Code of Practice (IS: 875: Part 3, 2015), the dynamic nature of the wind load is approximated by multiplying a gust amplification factor to equivalent static wind force. But, such approaches cannot assess stochastic and temporal variation of wind. Moreover, there have been several other limitations of this approach, viz. assumption of uniform wind flow pattern, disregard of flexibility of tall structures and difficulty in application to asymmetric structures. Also, in many cases, sufficient practical field data of spatial and temporal wind variation is not available. Hence, an attractive alternative is to generate artificial wind time history incorporating random nature of wind. It is well established that wind speed comprises of a mean wind speed component that varies with height and a gust wind component which represents fluctuations with respect to mean component. Most often, wind load is estimated considering alongwind component only (Spagnoli and Montanari 2013, Venanzi *et al.* 2015) by using Spectral Representation Method (SRM). However, direction of wind is an important parameter as the structural resistance is highly direction dependent. Gur and Chaudhuri (2014) obtained stochastic wind field considering wind directionality and associated coherence effect. The authors generated Artificial Wind Time History (AWTH) using the Fast Fourier Transform (FFT) and Kaimal's Power Spectral Density Function (PSDF). However, most of such studies considered the mean component of wind speed to be stationary. But, researches revealed that the mean component may be non-stationary during storms, typhoon or tornado (Chen and Letchford 2004). During passage of such strong winds, the traditional boundary layer profile of mean wind component with height becomes invalid and the wind field has to be simulated as non-stationary process (Chen and Letchford 2004, Kwon and Kareem 2009). In fact, numerous structural failures have been recorded due to tornado and typhoon in America, Japan, and recently in Peru. Hence, it becomes invariant to account for such power flashes of wind when addressing wind fragility assessment of tall structures. Thus, to investigate these aspects of wind field modeling, the present study explores fragility analysis by three Wind Field Models (WFM), viz. i) WFM I: with stationary mean component and alongwind gust component using Kaimal's PSDF (Effect of wind directionality and coherence is not considered in this model); ii) WFM II: with stationary mean component but considering wind directionality and coherence effect; the approach described in Gur and Chaudhuri (2014) has been adopted, iii) WFM III: this is an extension of WFM II but considering non-stationary mean component as per Chen and Letchford (2004). In the present paper, the wind fragility and risk analysis have been carried out using these three WFMs in separate modules. The importance of non-linear structural analysis in fragility evaluation has been also demonstrated.

Thus, the primary objective of this study is: i) to propose a computationally efficient wind fragility and risk assessment procedure of tall building structure in the MLSM based RSM framework; ii) to explore and compare various artificially generated WFMs considering effect of wind directionality, coherence and non-stationary nature of wind in separate modules, and iii) to compare the difference between linear and non-linear response analysis in the risk assessment procedure.

2. Wind fragility and risk analysis

Risk assessment is used in many situations with the general intention to quantify overall probability of failure of structure that specific response levels (e.g., maximum displacement of building, interstorey drift, etc.) are exceeded during its lifetime. Thus, risk can be defined as (Das 1988)

$$P_f = \int_0^{2\pi} \int_{V_{min}}^{V_{max}} P[\delta(\Theta) > \delta_{allowable} | v, \theta] f(v, \theta) dv d\theta \quad (1)$$

where, $P[\delta(\Theta) > \delta_{allowable} | v, \theta]$ also referred as fragility, is the probability that dynamic response, $\delta(\Theta)$ will exceed a user specific allowable threshold response ($\delta_{allowable}$) when subjected to wind with speed v and wind incidence angle θ ; V_{max} and V_{min} are the possible maximum and minimum mean wind speed specific to a site; Θ is a vector of random parameters. $f(v, \theta)$ is the joint Probability Density Function (PDF) of v and θ representing site specific hazard. In many literatures, effect of wind incidence angle is not considered in risk analysis, though, it is now established that it has a major impact on wind response analysis of a structure. The double integral of Eq. (1) is executed considering failure domain $g(v, \theta): [\delta(\Theta) - \delta_{allowable}] \geq 0$ encompassing all the possible combinations of hazard. The hazard PDF is obtained as: $f(v, \theta) = P_{v|\theta} P_\theta$ following Repetto and Solari (2004), where $P_{v|\theta}$ is the probability of occurrence of speed v when wind attacks at an angle θ , P_θ is the probability that wind blows from the direction θ with non-zero velocity. The possible wind speed range is divided into N_v number of segments. Also, angle of 2π is divided into N_θ numbers of wind incidence angle sectors. $P_{v|\theta}$ and P_θ are obtained based on the statistical data of wind speed and wind direction, specific to a site where structure is situated. Adopting Weibull distribution for wind speed, $P_{v|\theta}$ can be obtained as

$$P_{v|\theta} = \left\{ \exp\left[-\left(\frac{(i-1)\Delta v}{c_h}\right)^{k_h}\right] - \exp\left[-\left(\frac{i\Delta v}{c_h}\right)^{k_h}\right] \right\}; \quad \forall i \in N_v \quad (2)$$

where, Δv is speed step; c_h and k_h are the distribution parameters.

In the present paper, maximum deflection of the building is considered as the response quantity,

i.e. $\delta(\Theta) = \max\{Y(\Theta, t)\}$, where, \mathbf{y} denotes vector of deflections, which is obtained by solving the following equation

$$[\mathbf{M}]\{\ddot{\mathbf{Y}}(\Theta, t)\} + [\mathbf{C}]\{\dot{\mathbf{Y}}(\Theta, t)\} + [\mathbf{K}]\{\mathbf{Y}(\Theta, t)\} = \mathbf{F}(\Theta, t) \quad (3)$$

In the above, $[\mathbf{M}]$, $[\mathbf{C}]$ and $[\mathbf{K}]$ are the global mass, damping and stiffness matrix of the system, respectively. \mathbf{y} ; $\ddot{\mathbf{Y}}(\Theta, t)$, $\dot{\mathbf{Y}}(\Theta, t)$ and $\mathbf{Y}(\Theta, t)$ are acceleration, velocity and displacement vector of structure due to stochastic wind load $\mathbf{F}(\Theta, t)$, t denotes time. Thus, $\mathbf{Y}(\Theta, t)$ is obtained by linear/non-linear time history analysis of finite element model of the tall building. The randomness in the parameters Θ is conventionally incorporated by performing a MCS.

It may be noted at this point that to estimate risk by Eq. (1) using direct MCS, finite element model of structure is to be executed for nonlinear time history analysis for as many times as is the number of statistical simulation samples for all possible realization of hazard levels. Finally, the convolution integral is to be evaluated to compute risk. Thus, several re-analyses and interlinking between finite element analysis software and the MCS engine are generally involved in the MCS based risk analysis approach. Hence, risk evaluation by the MCS will be computationally prohibitive for tall buildings. Thus, the present paper explores efficient metamodelling approach in risk analysis to make the procedure computationally efficient. In doing so, response of nonlinear time history analysis of finite element model of tall building structure is approximated in terms of uncertain parameters (Θ) by means of RSM equations. This will not only reduce the complexity of analysis but also reduce computational time requirement. In fact, the task of several repetitive nonlinear time history analysis of finite element model is partly replaced by the equivalent metamodel by the proposed approach. The next section describes the procedure of risk analysis by the proposed metamodelling framework.

3. Risk analysis in metamodelling framework

A metamodel primarily uncovers analytically complicated or an unknown relationship between several inputs and desired output through simple mathematical model in which the response function is replaced by a simple function (often polynomial) that is fitted to a dataset through carefully selected points, referred as Design of Experiments (DOE). Polynomial metamodelling approach is primarily hinged on the concept of the LSM based RSM (Myers and Montgomery, 1995), where the best fitted response surface is obtained by minimizing square of errors associated with the DOE points. It will be informative to first discuss the background of LSM based RSM, then, the difference of the LSM with the proposed MLSM is presented.

3.1 The LSM based RSM

In the present paper, the dynamic response of the structure $\delta(\Theta)$ is approximated by the RSM based metamodelling technique as function of uncertain parameters, Θ . The conventional RSM is hinged on the concept of the LSM. The LSM based RSM performs a global approximation for a scatter data set. Given, n_l response values y_{nl} , corresponding to n_l numbers of observed input data x_{ij} (denotes the i^{th} observation of the regressor x_j in the DOE), the relationship between the response, \mathbf{y} and the regressor variables, $\mathbf{X}=[x_1, x_2, \dots, x_p]$ can be expressed by the following

$$\mathbf{y} = \mathbf{Q}\boldsymbol{\beta} + \boldsymbol{\varepsilon} \quad (4)$$

In the above multi-variable non-linear regression model \mathbf{y} , \mathbf{Q} , $\boldsymbol{\beta}$ and $\boldsymbol{\varepsilon}$ are the response vector, the design matrix containing the input data from the DOE, the unknown coefficient vector and the error vector, respectively. Typically, the quadratic polynomial form used in the RSM is as below

$$\hat{y} = \Phi(\mathbf{X}) = \beta_0 + \sum_{i=1}^{lk} \beta_i x_i + \sum_{i=1}^{lk} \sum_{j=1}^{lk} \beta_{ij} x_i x_j = \mathbf{Q}\boldsymbol{\beta} \quad (5)$$

where, \hat{y} is the predicted response, Φ represents a function, lk is the total number of regressors, (\mathbf{X}). The unknown polynomial coefficient vector is obtained by minimizing an error norm which represents the sum of the squares of errors as

$$\begin{aligned} Err_y &= \sum_{i=1}^{nl} \left(y_i - \beta_0 - \sum_{i=1}^{lk} \beta_i x_i - \sum_{i=1}^{lk} \sum_{j=1}^{lk} \beta_{ij} x_i x_j \right)^2 \\ &= (\mathbf{y} - \hat{\mathbf{y}})^T (\mathbf{y} - \hat{\mathbf{y}}) = (\mathbf{y} - \mathbf{Q}^* \boldsymbol{\beta})^T (\mathbf{y} - \mathbf{Q}^* \boldsymbol{\beta}) \end{aligned} \quad (6)$$

In the above, \mathbf{Q}^* is the design matrix whose elements are evaluated at the observed scatter data set. The least squares estimate of ($\boldsymbol{\beta}$) is then obtained as (Myers and Montgomery 1995)

$$\boldsymbol{\beta} = [\mathbf{Q}^{*T} \mathbf{Q}^*]^{-1} \mathbf{Q}^{*T} \mathbf{Y} \quad (7)$$

Once, the polynomial coefficients ($\boldsymbol{\beta}$) are evaluated by the above equation, the response (\mathbf{y}) can be readily evaluated for any set of input parameters.

Though, the LSM based RSM is a widely used conventional method, possibility of inclusion of error by the LSM has been reported by various researchers (Kim *et al.* 2005, Goswami *et al.* 2016). This may be due to its characteristics of global approximation. In this regard, a comparatively new Moving Least Squares Method (MLSM), which is based on 'moving' and 'local' approximations, seems to be more elegant, and presented in the next section.

3.2 The MLSM based RSM

The LSM based RSM yields expression which is invariant for the whole domain of variation of input variables. As a result, zone-wise variation cannot be

captured by the LSM. On the other hand, the MLSM, being a local approximation procedure, provides more accurate prediction of dynamic response by capturing zone-wise variations of the actual responses. The MLSM based RSM is basically a weighted LSM that has varying weight functions with respect to the position of approximation (Taflanidis and Cheung, 2012). The weight associated with a particular sampling point x_i decays as the prediction point \mathbf{x} moves away from \mathbf{x}_i . The weight function is defined around the prediction point \mathbf{x} and its magnitude changes with \mathbf{x} . The modified error norm $Err_y(\mathbf{X})$ can be defined as the sum of the weighted errors by modifying Eq. (6) as (Kim *et al.* 2005)

$$\begin{aligned} Err_y(\mathbf{X}) &= (y - \hat{y})^T \mathbf{W}(\mathbf{X})(y - \hat{y}) \\ &= (y - \mathbf{Q}^* \boldsymbol{\beta})^T \mathbf{W}(\mathbf{X})(y - \mathbf{Q}^* \boldsymbol{\beta}) \end{aligned} \quad (8)$$

where, $\mathbf{W}(\mathbf{X})$ is a diagonal Weight matrix and it depends on the location of the associated approximation point of interest (\mathbf{x}). ' $\mathbf{W}(\mathbf{x})$ ' is obtained by utilizing a weighting function as (Taflanidis and Cheung 2012)

$$\begin{aligned} w(\mathbf{x} - \mathbf{x}_i) &= w(\mathbf{d}) \\ &= \begin{pmatrix} e^{-\left(\frac{d}{c\Gamma}\right)^{2k}} & -e^{-\left(\frac{1}{c}\right)^{2k}} \end{pmatrix} / \begin{pmatrix} 1 - e^{-\left(\frac{1}{c}\right)^{2k}} \end{pmatrix}, \text{if } \mathbf{d} < \Gamma; \text{else } 0 \end{pmatrix} \quad (9)$$

where, Γ defines domain of the influence of point \mathbf{x}_i ; \mathbf{d} is the Euclid distance between sampling point \mathbf{x}_i and prediction point \mathbf{x} ; and c, k are free parameters to be selected for better efficiency which are taken here as 0.4 and 1.0, respectively (Taflanidis and Cheung 2012). The weight matrix $\mathbf{W}(\mathbf{x})$ can then be constructed by using the weight functions in diagonal terms as below

$$\mathbf{W}(\mathbf{x}) = \begin{bmatrix} w(x - x_1) & 0 & \dots & 0 \\ 0 & w(x - x_2) & \dots & 0 \\ \dots & \dots & \dots & \dots \\ 0 & 0 & \dots & w(x - x_n) \end{bmatrix} \quad (10)$$

Now, the coefficient vector $\boldsymbol{\beta}(\mathbf{X})$, which is also a function of regressor (\mathbf{X}) can be obtained by the matrix operation as below (Kim *et al.* 2005) which is analogous to Eq. (7)

$$\boldsymbol{\beta}(\mathbf{X}) = [\mathbf{Q}^{*T} \mathbf{W}(\mathbf{X}) \mathbf{Q}^*]^{-1} \mathbf{Q}^{*T} \mathbf{W}(\mathbf{X}) \mathbf{Y} \quad (11)$$

Thus, unlike the LSM, the response surface approximation by the MLSM will change for every realization of \mathbf{X} to capture minute localized variations. In the present paper, the dynamic response δ is approximated in terms of vector of random variable Θ by the MLSM based RSM as $\delta = \Phi(\Theta)$, where Φ is the polynomial function defined by Eq. (5).

3.3 Risk and fragility estimation in the MLSM based RSM framework

The scheme of the proposed fragility and risk estimation method by the MLSM based RSM is shown in Fig.1. At first, the MLSM based approximation of δ in term of Θ is obtained. To do so, N_r numbers of realizations of the random parameter vector Θ is generated by the Uniform Design (Fang *et al.* 2004) scheme and the DOE is constructed. Thus, the design matrix \mathbf{Q}^* is of $N_r \times n_k$ dimension, where, n_k is the total number of involved uncertain parameters. Once, an explicit functional form of δ is achieved, the MCS is implemented over this MLSM generated expression to evaluate fragility $Fr(v, \theta)$ by the following equation

$$Fr(v, \theta) = P[\{\delta = \Phi(\Theta)\} > \delta_{allowable} | v, \theta] = (n_f / N) \quad (12)$$

where, $\delta_{allowable}$ is a user specific maximum allowable response. N is the total number of MCS samples and n_f is the number of simulations for which

$$[\delta = \Phi(\Theta)] > \delta_{allowable} \quad (13)$$

Once, the fragility is estimated for various sets of v and θ , using the joint PDF of hazard $f(v, \theta)$ the Risk is obtained as

$$P_f = \sum_{v=V_{min}}^{V_{max}} \sum_{\theta=0}^{2\pi} Fr(v, \theta) f(v, \theta) \quad (14)$$

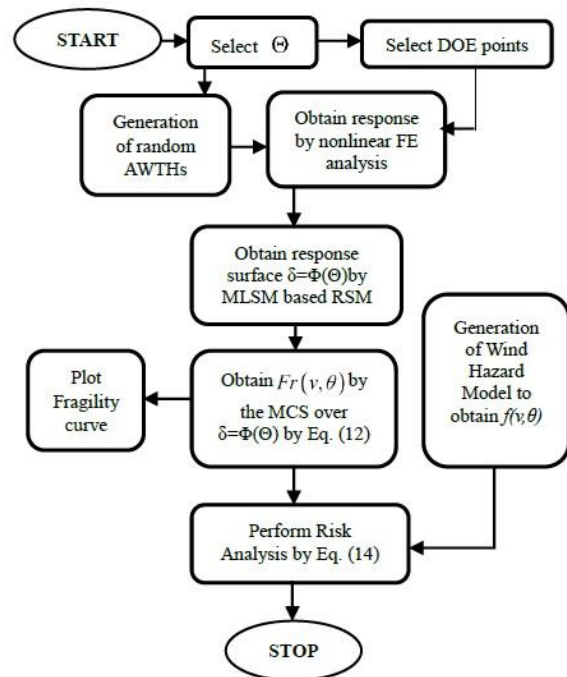


Fig. 1 Flow chart to perform fragility and risk analysis by the proposed approach

In short, the implementation steps (Fig. 1) are as follows; i) Selection of Θ , ii) Uncertainty quantification for Θ and construction of DOE, iii) Generation of thirty sets of AWTH at each DOE, iv) Non-linear time history analysis of structure to obtain maximum displacement using finite element (FE) software; v) Generation of MLSM based metamodelling expression of $\delta = \Phi(\Theta)$ by Eqs. (5) and (11), vi) Validation of the MLSM yielded expression with actual FE predicted response, vii) Incorporation of uncertainty in the analysis by the MCS operated over this MLSM generated explicit equation to estimate fragility for different $\delta_{allowable}$, ν and θ by Eq. (12), viii) Estimation of hazard for θ and ν and ix) Estimation of risk by Eq. (14). The approach is general and is applicable for any structure. Since, the MLSM based RSM partly replaces the MCS, computational efficiency of the proposed approach is expected to be more than the conventional full MCS based approach. At the same time, application of the MLSM in place of the LSM preserves the accuracy.

4. Generation of AWTH for wind speed

Accuracy of risk analysis largely depends on the proper estimation of wind load. $F(\Theta, t)$ of Eq. (3) is obtained by generating AWTH for wind speed and then wind force. Three WFM's have been investigated in the present study, viz. WFM I, WFM II and WFM III, which are detailed in subsequent sections.

4.1 Wind Field Model I (WFM I)

The Weighted Amplitude Wave Superposition (WAWS) method (Shinozuka and Jan 1972) using Kaimal's PSDF is referred in this paper as WFM I. The wind speed can be derived from a mean component $v(z)$ which is function of height z only and a gust component $v(t)$ which represents zero mean temporal variation of wind. Thus, wind speed can be expressed as

$$v_t(z, t) = v_n(z) + v(t) \quad (15)$$

The mean wind speed profile can be obtained by Hellman's power law as (Simiu and Scanlan 1986)

$$v_n(z) = v_g \left(\frac{z}{z_g} \right)^{1/\alpha} \quad (16)$$

where, v_g is the gradient wind speed at gradient height z_g and α is the power law exponent. Kaimal's PSDF (Kaimal *et al.* 1972) is adopted to simulate the gust component for alongwind turbulence as

$$\begin{aligned} S_v(\Omega, z) &= (1/2)(1/2\pi) 200 u_*^2 (z/V(z)) \\ &\times \left(1 / \left[1 + 50 / (\Omega |z| / 2\pi V(z)) \right]^{5/3} \right) \end{aligned} \quad (17)$$

where, $S_v(\Omega, z)$ is the Kaimal's PSDF, Ω is the frequency

in rad/s, V is the wind speed (in m/s) at elevation z , ' u_* ' is the shear velocity of wind flow which is obtained as (Ambrosini *et al.* 2002)

$$u_* = k_n V / \ln(z / z_o) \quad (18)$$

In the above, k_n is the von Karman constant (equal to 0.4), and z_o is the roughness length of the surface which depends on the surface properties (taken as 0.01 for smooth surface). Using the WAWS method, $v(t)$ is simulated as one-variate, one dimensional, homogeneous Gaussian random process (Spanos 1980) as

$$v(t) = \sqrt{2} \sum_{i=1}^{N_\Omega} \left[2S_v(V, \Omega) \Delta\Omega \right]^{0.5} \cos(\Omega t + \psi_i) \quad (19)$$

In above, ψ_i are random phase angles uniformly distributed between 0 and 2π , N_Ω is the total number of frequency intervals.

4.2 Wind Field Model II (WFM II)

In the dynamic wind analysis, it is necessary to generate wind field as spatially varying entity which considers wind directionality effect, as well. This has been one of the shortcomings of WFM I which is taken care of in WFM II. Accordingly, the second term of the RHS of Eq. (15) denoting gust component is replaced by $v(x, y, z; t)$ depicting gust is dependent on space coordinates, as well.

In order to include the spatial variation of wind turbulence in the vertical and the lateral directions, wind coherence models are adopted. Considering two points \mathbf{j} (coordinates x_j, y_j, z_j) and \mathbf{k} (coordinates x_k, y_k, z_k), the vertical and lateral coherence between these points are expressed as (Ambrosini *et al.* 2002, Harris 1990)

$$\begin{aligned} \eta_{jk}(\Omega, dx) &= \exp \left[-|\Omega| C_x dx / 2\pi V_{jk}(z) \right] \\ \gamma_{jk}(\Omega, dy, dz) &= \exp \left[-|\Omega| \sqrt{(C_y dy)^2 + (C_z dz)^2} / 2\pi V_{jk}(z) \right] \end{aligned} \quad (20)$$

where, $\eta_{jk}(\Omega, dx)$ and $\gamma_{jk}(\Omega, dy, dz)$ are the vertical and lateral wind coherence functions, respectively and dx, dy and dz are $|x_j - x_k|, |y_j - y_k|$ and $|z_j - z_k|$ respectively (in m), and $V_{jk}(z)$ is $0.5[V(z_j) + V(z_k)]$ m/s. C_x, C_y and C_z are constants that can be taken as 6.0, 10.0 and 16.0 respectively (Gur and Chaudhuri 2014). In order to incorporate wind directionality effect, the global coordinate system $(\mathbf{x}, \mathbf{y}, \mathbf{z})$ is transferred to a new coordinate system $(\mathbf{x}', \mathbf{y}', \mathbf{z}')$, relative to wind direction (θ) as

$$\begin{Bmatrix} \mathbf{x}' \\ \mathbf{y}' \\ \mathbf{z}' \end{Bmatrix} = \begin{pmatrix} \cos \theta & \cos(90^\circ - \theta) & \cos 90^\circ \\ \cos(90^\circ + \theta) & \cos \theta & \cos 90^\circ \\ \cos 90^\circ & \cos 90^\circ & \cos 0^\circ \end{pmatrix} \begin{Bmatrix} \mathbf{x} \\ \mathbf{y} \\ \mathbf{z} \end{Bmatrix} \quad (21)$$

The fluctuating component of the wind field is considered as one dimensional stationary Gaussian process. The complex cross spectral density matrix (CSDM) $S^o(\Omega)$ of the fluctuating component of wind can be expressed as (Popescu *et al.* 1998)

$$S^o(\Omega) = \begin{bmatrix} S_{11}^o(\Omega) & S_{12}^o(\Omega) & S_{13}^o(\Omega) & \cdots & S_{1n}^o(\Omega) \\ S_{21}^o(\Omega) & S_{22}^o(\Omega) & S_{23}^o(\Omega) & \cdots & S_{2n}^o(\Omega) \\ \vdots & \vdots & \vdots & \ddots & \vdots \\ S_{n1}^o(\Omega) & S_{n2}^o(\Omega) & S_{n3}^o(\Omega) & \cdots & S_{nn}^o(\Omega) \end{bmatrix} \quad (22)$$

The diagonal elements of the CSDM, S_{jj}^o are the PSDFs which are real and non-negative functions of Ω . The off-diagonal elements of CSDM, S_{ij}^o are the cross PSDFs which are complex functions of Ω . The elements of CSDM is taken as (Chen and Letchford 2004)

$$S_{jj}^o = S_j(\Omega), \quad \forall j, k \in n: j = k; \quad (23)$$

$$S_{jk}^o = \sqrt{S_j(\Omega)S_k(\Omega)}\eta_{jk}\gamma_{jk}, \quad \forall j, k \in n: i \neq j$$

This CSDM matrix is a Hermitian matrix. Hence, it can be factorized into upper and lower triangular matrix by using Cholesky's method as

$$S^o(\Omega) = H(\Omega)H^{*T}(\Omega) \quad (24)$$

where, $H(\Omega)$ is a lower triangular matrix which can be defined as

$$H_{jk}(\Omega) = |H_{jk}(\Omega)|e^{i\theta_{jk}(\Omega)}, \quad \forall j \in n, \quad \forall k \in n-1, j > k; \quad (25)$$

$$\theta_{jk}(\Omega) = \tan^{-1} \left(\frac{\text{Im}[H_{jk}(\Omega)]}{\text{Re}[H_{jk}(\Omega)]} \right)$$

Finally, $v(x, y, z; t)$, $i=1,2,\dots,n$, can be simulated using FFT as (Brigham 1988, Gur and Chaudhuri 2014)

$$v_j^{(i)}(p\Delta t) = \text{Re} \left\{ \sum_{q=1}^i \sum_{l=0}^{M-1} B_{jql} \exp[ilp(2\pi/n)] \right\}, \quad (26)$$

$$\forall j \in n, \quad \forall p \in M-1, \quad l = \Gamma-1$$

$$B_{jql} = 2 |H_{jq}(l\Delta\Omega)| \sqrt{\Delta\Omega} \exp[-i\theta_{jq}(l\Delta\Omega)] \exp[i\phi_{ql}^{(i)}]$$

with $\Delta\Omega = \Omega_u/\Gamma$, $\Delta t = 2\pi/M\Delta\Omega$, $M=2\Gamma$, $\Delta\Omega = \Omega_u/N$ ϕ_{ql} is the random phase angle uniformly distributed over 0 to 2π and Ω_u is the upper cut frequency.

4.3 Wind Field Model III (WFM III)

In this section, the WFM II is further extended to incorporate non-stationary wind effect. The mean wind speed component v_n of Eq. (15) becomes non-stationary stochastic when structure is subjected to sudden downbursts of storm. Thus, the first term of the RHS denoting mean wind speed component is replaced by $v_n(z,t)$. Chen and

Letchford (2004) calculated $v_n(z,t)$ as: $v_n(z,t) = v_n(z) \times f(t)$, where $f(t)$ is a time modulating function. $v_n(z)$ is estimated by using Eq. (16). $f(t)$ is adopted from Chen *et al.* (2012) that is based on the Holmes' empirical model (Holmes and Oliver 2000), which agrees well with radar observations of Hjelmfelt (1988). According to this, the radial profile of horizontal radial downburst wind speed $V_r(r)$ as function of radial distance r is given by

$$V_r(r) = \begin{cases} V_{r,max} \times (r - r_{max}), & 0 \leq r \leq r_{max} \\ V_{r,max} \times \exp\left(-\left[(r - r_{max})/R_r\right]^2\right), & r > r_{max} \end{cases} \quad (27)$$

where, $V_{r,max}$ is the maximum velocity in the profile; R_r is a radial length scale; r_{max} is the radial distance from the storm center at which the maximum velocity is achieved; r is measured from the stagnation point. The storm is assumed to move forward along its straight track with the translation speed V_t . The offset distance of the downburst track from the observing point is e . At time $t=0$, say the coordinate of the observing point is (d_o, e) . So, after time t , the coordinate of observing point is $r = (d_o - V_t t, e)$. The radial jet velocity vector is then obtained by $V_r(t) = (r/|r|)V_r(|r|)$. Thus, the combined wind velocity vector is $V_c(t) = V_r(t) + V_t$. Then, the time function is defined by

$$f(t) = |V_c(t)| / \max |V_c(t)| \quad (28)$$

The PSDF of the gust component will also vary with time. Hence, Evolutionary Power Spectrum Density Function (EPSDF) must be used for modeling this non-stationary process. The PSDF of Eq. (17) is converted to the EPSDF in this case by applying a modulation function $a(z,t)$ used in Chen and Letchford (2004). Thus, the CSDM (Eq. (23)) and the gust (Eq. (26)) of the stationary process are modified as given below

$$S_{jj,NS}^o = |a_j(z,t)|^2 S_{jj}^o(\Omega) \quad (29)$$

$$S_{jk,NS}^o = |a_j(z,t)||a_k(z,t)| \sqrt{S_j(\Omega)S_k(\Omega)}\eta_{jk}\gamma_{jk}$$

$$v_{NS}(z,t) = a(z,t)v_j^{(i)}(z,p\Delta t) \quad (30)$$

4.4 Generation of Time History of Wind Force

The force of lift due to wind pressure will be negligible and only the effect of drag force is considered. Once, the AWTH for wind speed is generated by any of the WFM, the drag force due to wind pressure difference on the structure is estimated as

$$F_i(\Theta, x, y, z, t) = 0.5\rho[v_n + v(t)]^2 C_D A_i \quad (31)$$

where, F_i is the wind force at the i^{th} floor level at time t , C_D

is the drag coefficient, ρ is the density of air and A_i is the tributary area perpendicular to the wind flow direction at the i^{th} floor level.

5. Numerical study

A twenty storied reinforced concrete (RC) building (Fig. 2) is considered to elucidate the efficiency of the proposed approach. The length and width of the building is 30 m and 20 m, respectively in plan. The total height of the building above ground is 73.14 m with storey height 4 m each. Shear walls are located in the panel zones C1D1, C5D5, C1C2 and C4C5. The sectional elevation along line 1 is shown in Fig. 2(a).

The column dimension is varied as: (600 mm x 800 mm) for ground to 5th floor, (475 mm x 650 mm) for 6th to 10th floor, (450 mm sq.) for 11th to 17th floor and (400 mm sq.) for 18th floor to roof. The beams are considered as 450 mm x 750 mm for the first six floors and 450 mm x 600 mm for rest of the floors. The thickness of shear wall is 200 mm. These dimensions are obtained after designing the structure by Indian Standard specifications considering Dead Load, Live Load, Seismic Load and Wind Load. The dead load consists of self-weight of structural and non-structural members. The concrete grade is considered to be of M35 (i.e., the characteristic strength of concrete is 35 N/mm²) and the reinforcement steel grade is taken as TMT steel having yield strength of 500 N/mm². As the first task, AWTHs are generated by the WFM I, WFM II and WFM III, in separate modules. Considering building is located in suburban area, z_G and α are taken as 275 m and 7, respectively (ANSI A58.1-1982). In order to consider a larger variation of the approaching wind speed, the basic wind speed at the location is assumed to vary between 30 m/s to 80 m/s at an interval of 5 m/s based on Indian wind climatic condition. The value of θ in WFM II and WFM III is varied from 0° to 90° at an interval of 15° considering symmetry of the structure. θ is considered as 0° when wind flows along the direction 3-3. For WFM III, r_{max} is taken as 1000, e as 150, V_r as 12 m/s and d_0 as 3200 (Chen and Letchford 2004). However, for more accurate estimation, last 50 years' statistical data of wind should be analyzed. The AWTH for wind speed is generated for all the three WFMs by developing MATLAB scripts. The wind force time histories are then obtained using Eq. (31). The value of C_D is assumed to vary in between 1.2 and 1.7 with an interval of 0.1 according to possible minimum and maximum range of C_D as per IS: 875:2015. However, more accurate estimation of C_D can be obtained by computational fluid dynamics analysis or by wind tunnel experiment. $E=5000\sqrt{35}=29580$ MPa as per IS: 456:2000. Wind speed and wind angle normally have more uncertainty levels compared to the other parameters. Thus, uncertainty in v and θ are considered at 20% CoV, whereas, uncertainty in other parameters is considered at 10% CoV. However, for more accurate values of mean and CoV a detailed statistical analysis may be made which is also dependent on specific site location, wind interference effect, degree of quality control in concrete production, etc. In this regard, one may

refer NBS special publication (Ellingwood *et al.* 1980). The uncertainty information about the parameters (⊕), considered in this study, are presented in Table 1.

Table 1 Uncertainty information about the random parameters

| Parameter | Distribution | Mean | CoV |
|------------------|--------------|-------------|------|
| C_D | Normal | 1.2-1.7 | 10% |
| v | Weibull | 30-80 m/sec | 20 % |
| E | LogNormal | 29.58 GPa | 10% |
| z_g | Normal | 275 m | 10% |
| θ | Uniform | 0°-90° | 20% |
| α | Normal | 7 | 10% |
| r_{max} | Normal | 1000 | 10% |
| e | Normal | 150 | 10% |
| V_r | Normal | 12 m/s | 10% |
| d_0 | Normal | 3200 | 10% |

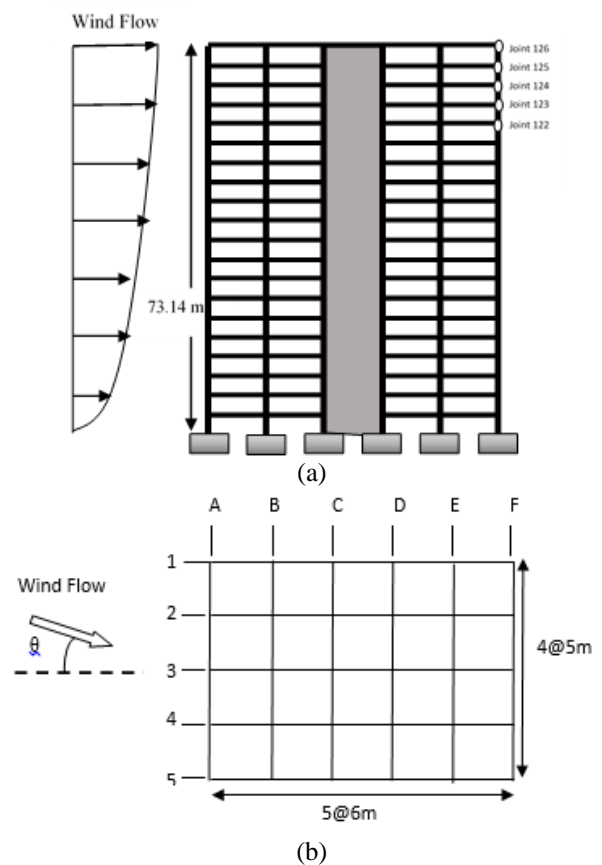


Fig. 2 (a) Sectional Elevation (along line 1) and (b) Plan of building

The AWTHs for wind speed at the topmost node (joint 126) by the three WFM are presented in Figs. 3-5, respectively. It can be observed that the AWTH by the WFM I show lesser mean than WFM II; however, WFM I yields higher fluctuations with respect to mean than WFM II. The AWTH by WFM III (Fig. 5) shows different trend than WFM I and WFM II, owing to its non-stationary mean component of wind speed. The AWTH by WFM III shows two dominant peaks due to sudden downbursts of wind.

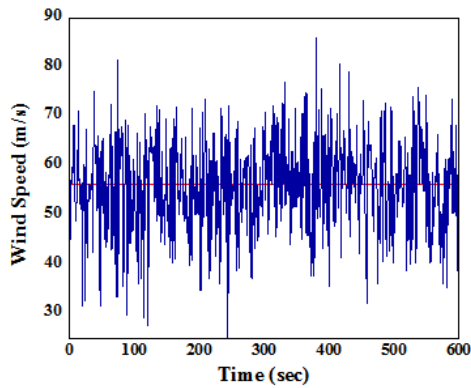


Fig. 3 The AWTH by WFM I at Joint 126

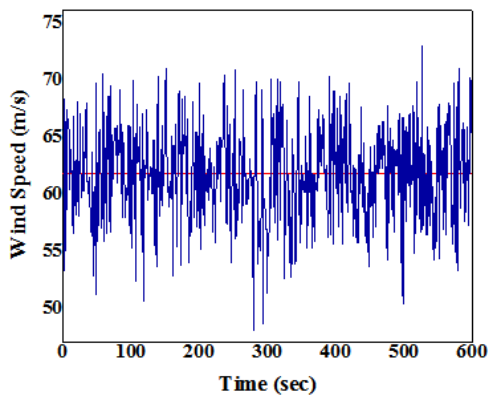


Fig. 4 The AWTH by WFM II at Joint 126

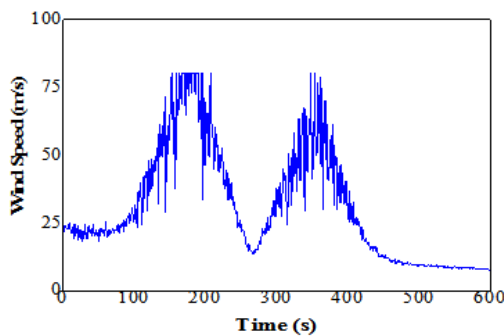


Fig. 5 The AWTH by the WFM III at Joint 126

The dynamic response of the building under artificially generated wind force time histories has been obtained by non-linear time history analysis (NLTHA) using commercial software SAP2000NL. The stress-strain characteristic of concrete is considered as per Mander’s confined model (Mander and Priestley 1988) for the column members and unconfined concrete model for the beam members. For reinforcing steel, the simple stress strain model with isotropic strain hardening behaviour is considered. These models are readily available as in-built model in the software. The beams and columns are characterized by the lumped plasticity model. For this purpose, the nonlinear hinges are assigned at the beam and column ends. The beams are modeled with moment hinges (M3) whereas the columns are modeled with axial-moment (P-M3) interacting hinges. Auto hinges are assigned according to the tables of FEMA 356 (2000). The NLTHA is carried out by Hiber-Hughes-Taylor (HHT) integration scheme. After executing the NLTHA, the maximum displacement values are obtained representing the structural demand. A deflected shape of the building obtained by the NLTHA using WFM II is presented in Fig. 6.

To visualize the effect of nonlinearity, a parametric study is made in terms of time-history of maximum horizontal displacements at five selected nodes. For the sake of comparison, the linear time history analysis results are also shown side by side. Nodal displacement time histories as obtained using WFM II are plotted in Figs. 7 and 8. Fig. 7(a) shows the horizontal displacement time-histories yielded by linear dynamic analysis and Fig. 7(b) shows displacement time-histories by the non-linear time-history analysis. v and θ are considered to be 50 m/s and 0° to produce these results. It can be observed that the maximum displacement values by the nonlinear analysis (Fig. 7(b)) are consistently higher than the linear analysis case (Fig. 7(a)).

The nodal displacement time-histories yielded by WFM III are presented in Figs. 8(a) and 8(b) for linear and non-linear dynamic analysis, respectively.

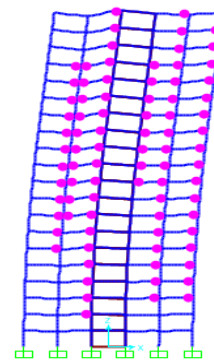


Fig. 6 Deflected shape of the building for WFM II by non-linear time-history analysis

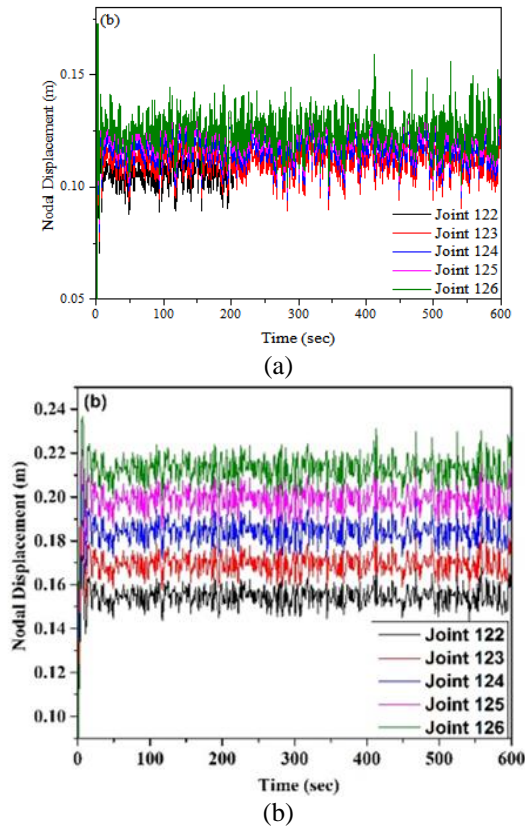


Fig. 7 (a) Nodal displacement time histories by linear dynamic analysis for WFM II and (b) Nodal displacement time histories by non-linear dynamic analysis for WFM II

The trend of time-displacement signature by WFM III is distinctly different from that by WFM II. However, the displacement values by the non-linear dynamic analysis case (Fig. 8(b)) is observed to be more than the linear dynamic analysis result (Fig. 8(a)) in this case, as well. Thus, the maximum displacement values by the nonlinear analysis being consistently higher than the linear analysis by both the WFMs, it can be inferred that the linear dynamic analysis may not be conservative for fragility analysis.

Further, it can be observed from these Figs. that both in linear and non-linear cases, the WFM III yield lesser displacement values than by the WFM II. Similar observation has been reported in Chen *et al.* (2007) as well by comparing stationary and non-stationary wind models, which was also validated by them through field measurements.

The results of NLTHA are now used to approximate the maximum displacement response by the MLSM based RSM. But, before such approximation is used in fragility evaluation, it is essential to check the validity of the fitted MLSM based response surface. In Fig. 9, the displacement response surface obtained by the MLSM is presented using WFM II. The actual NLTHA results are also shown by ‘black dots’ and the LSM based predictions are shown by ‘black asterisks’. It can be clearly observed that the NLTHA

results fit well with the response surface; whereas, the LSM based predictions are far away than the NLTHA result points. The accuracy by the MLSM based RSM is further presented by a bar diagram in Fig. 10. The deflection by the NLTHA, the LSM and the MLSM are presented in the same figure for different realizations of Θ other than the DOE points. Here also, the accuracy by the MLSM over conventional LSM is pertinent. It can be further observed that the LSM predictions are consistently on the higher side.

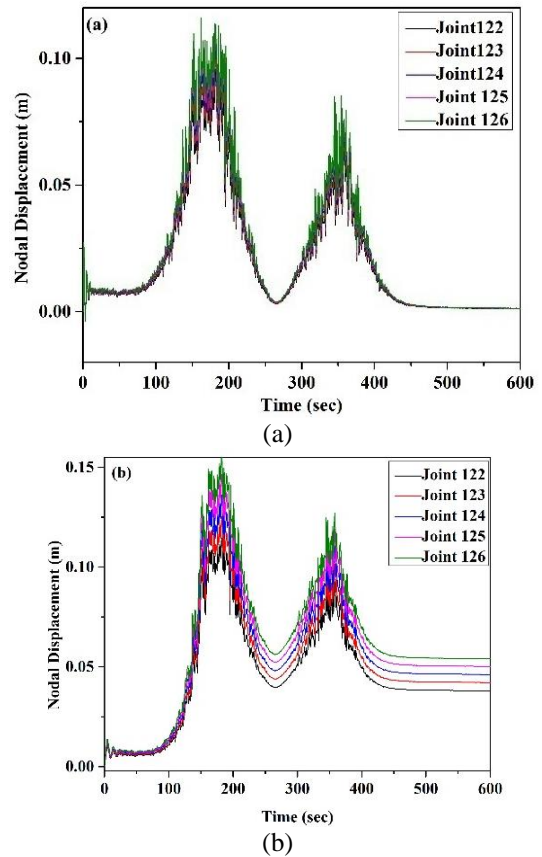


Fig. 8 (a) Nodal displacement time histories by linear dynamic analysis for WFM III and (b) Nodal displacement time histories by non-linear analysis for WFM III

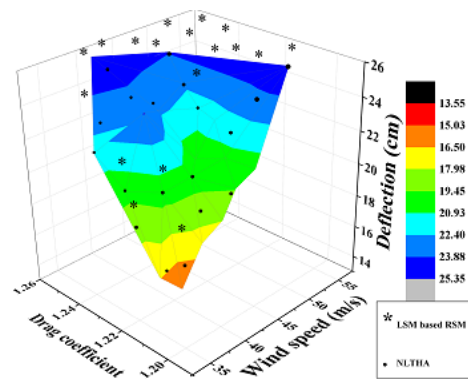


Fig. 9 The Response surface by the MLSM

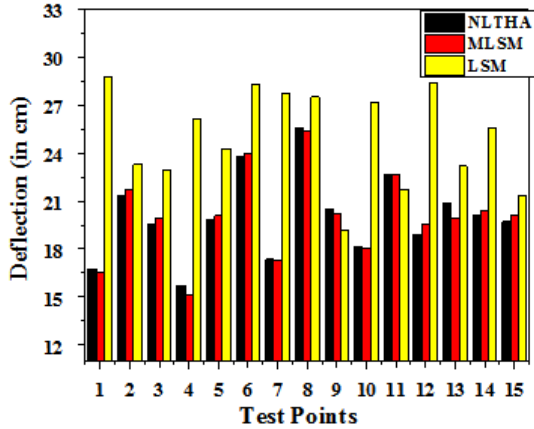


Fig. 10 Comparison of the MLSM and LSM predictions with the NLTHA response

The fragility analysis is now performed over the generated RSM expression by using direct MCS. The MCS converges at one lac simulation. In this regard, a convergence study is presented in Fig. 11. The fragility curves obtained by the WFM I, WFM II and WFM III using the proposed MLSM based RSM (referred as ‘Proposed’ in the Figs) are presented in Figs. 12-14, respectively. The fragility ordinates as obtained by the LSM and the conventional full direct MCS approach are also presented in the same figures. In WFM I case, the fragility curves have been developed for different allowable displacement levels ($\delta_{allowable}$) of the building, viz. H/500, H/350, H/250 and H/100, where H is the total height of the building. It may be noted that WFM I reckons to alongwind behavior only; whereas, WFM II and WFM III are spatially varying wind fields. Hence, fragility curves are plotted for various angles of wind incidence for WFM II and WFM III cases. It can be observed from Figs. 12 to 14 that the proposed MLSM based RSM yields fragility curves are in good conformity with the well-established full direct MCS predicted fragility curves in all the cases. However, the fragility points by the LSM based approach are far away than the direct MCS yielded fragility points. Thus, the proposed MLSM based approach is more accurate than the conventional LSM based approach when compared to the direct MCS results as reference.

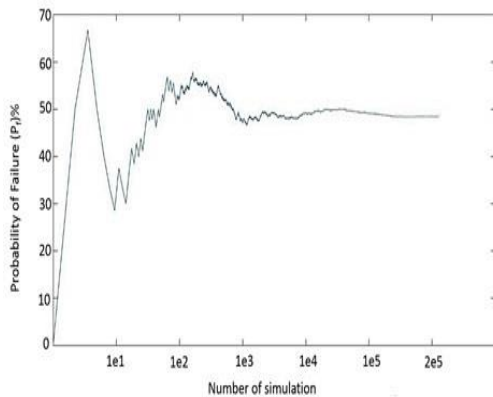


Fig. 11 Convergence study by the MCS

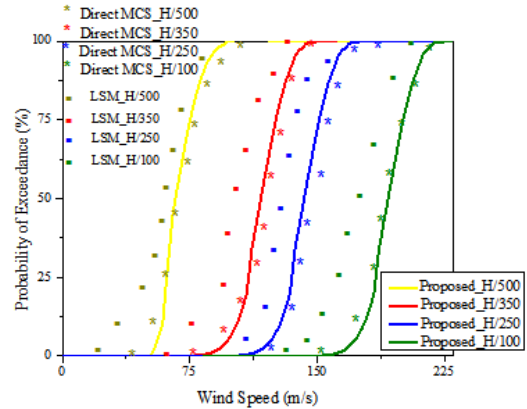


Fig. 12 The fragility curves for the WFM I case

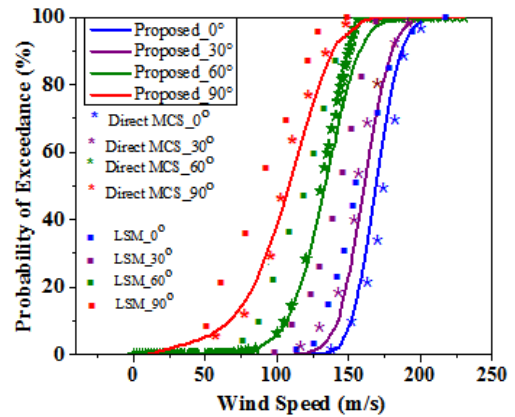


Fig. 13 The fragility curves for the WFM II case

In fact, the errors noted in Figs. 9 and 10 by the LSM propagate in the fragility analysis, yielding large deviation from the direct MCS results.

The fragility curves show that there is only 0.1% chance of failure at 50 m/s wind speed by WFM I. However, the wind incidence angle is by default 0° for this load model. The probability of failure by the WFM II is 9% for the same wind speed, but this occurs when wind incidence angle is 90°. By WFM III, the probability of failure is 1% for the same wind speed and same wind incidence angle. Thus, the application of WFM I may not be always conservative in fragility point of view. In other words, fragility analysis by WFM I may underestimate the prevailing failure risk. By observing Figs. 14 and 15, it can be inferred that 90° is the most critical wind incidence angle for the considered structure. It may be further observed from Figs. 12 -14 that the LSM yielded probability of exceedance is always in higher side. Thus, in the present case the LSM overestimates the probability of failure.

It may be noted at this point that the full simulation approach took 161 hours to yield a fragility curve for a single case with one 8 GB RAM processor computer. On the other hand, the proposed MLSM based RSM yields the fragility curve for the same case by only 7 minutes (average) once the MLSM based explicit expression is

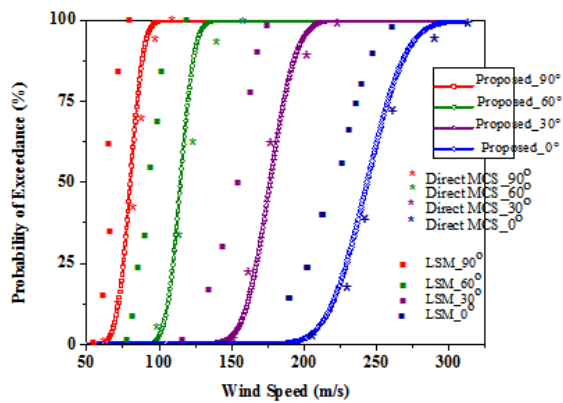


Fig. 14 The fragility curves for the WFM III case

generated. The total time taken starting from generation of AWTH, construction of DOE, analysis of the FEM model in SAP, generation of the MLSM based expression to fragility analysis for the above case is only 3.5 hours. This establishes the computational efficiency of the proposed MLSM based approach over conventional full simulation approach.

6. Risk analysis

In this section, the overall risk of failure of the building is presented for different WFM cases as calculated by Eq. (14). The probability of occurrence of a specific wind speed magnitude in a particular site is represented by wind hazard models. The wind hazard model is developed assuming Weibull distribution for wind speed by adopting Eq. (2). The values of the distribution parameters are adopted from the study of Sarkar *et al.* (2011) and Sarkar *et al.* (2017) for three major commercial cities in India having different wind climate conditions, namely, Kolkata, Bombay and Ahmedabad. The directional dependency of the wind speed is assumed to be uniformly distributed. The values of $P_{v|0}$ and P_0 are accordingly obtained using the procedure in Repetto and Solari (2004). The risk of failure of the considered building by the WFM II and WFM III in these cities is summarized in Table 2. It may be observed that WFM II yields more risk than that predicted by WFM III. This observation is in conformity with the trend of fragility curves. Among the three cities, Kolkata is having the maximum wind risk owing to its meteorological position. It can be further observed from Table 2 that the proposed MLSM based approach predicted risks are in close conformity with the direct MCS results in most cases. Whereas, the risks predicted by the LSM seems to be erroneous when compared to the full MCS approach as reference.

Table 2 Wind Risk Analysis by the three WFMs for the three cities in India

| City | WFM | Approach | Risk |
|-----------|---------|----------|-------|
| Kolkata | WFM II | LSM | 10.5% |
| | | MLSM | 5.17% |
| | | MCS | 4.91% |
| | WFM III | LSM | 8.2% |
| | | MLSM | 4.15% |
| | | MCS | 4.01% |
| Bombay | WFM II | LSM | 9% |
| | | MLSM | 3.91% |
| | | MCS | 3.71% |
| | WFM III | LSM | 5.3% |
| | | MLSM | 3.5% |
| | | MCS | 3.22% |
| Ahmedabad | WFM II | LSM | 7.86% |
| | | MLSM | 3.18% |
| | | MCS | 2.91% |
| | WFM III | LSM | 5.5% |
| | | MLSM | 2.95% |
| | | MCS | 2.21% |

7. Conclusions

An efficient wind fragility and risk analysis procedure in the MLSM based metamodelling framework is presented. The proposed approach is elucidated by a twenty storied RC building. The proposed approach is computationally efficient than the conventional full simulation approach of fragility analysis. At the same time, the proposed approach is accurate as well when compared with the conventional LSM based RSM taking full MCS solutions as the reference. In this regard, the error in the results yielded by the conventional LSM based RSM is clearly notable. The fragility analysis has been performed with stochastic AWTH generated by three WFMs, which consider the effect of wind incidence angle, wind coherence effects and non-stationary component of mean wind speed in separate modules. The probabilistic wind risks for three major cities in India have been investigated. After exploring various WFMs it is clear that conventional WFM I approach disregarding coherence and wind directionality effect may lead to unsafe predictions. In this regard, WFM II is the most conservative. Also, the results indicate that non-linear time history analysis must be done in fragility analysis, since linear dynamic analysis is observed to underestimate the structural response in the present case. The proposed MLSM based fragility analysis procedure is a general one and can be applicable for any structure. However, WFMs should be suitably updated to cater special wind-structure interaction aspects, like buffeting or lock-in effect.

References

- Ambrosini, R.D., Riera, J.D. and Danesi, R.F. (2002), "Analysis of structure subjected to random wind loading by simulation in the frequency domain", *Probab. Eng. Mech.*, **17**, 233-239.
- ANSI A58.1 (1982), *Design Loads For Buildings And Other Structures*, Minimum, American National Standards Institute.
- Bhattacharjya, S. and Chakraborty, S. (2011), "Robust optimization of structures subjected to stochastic earthquake with limited information on system parameter uncertainty", *Eng. Optimiz.*, **43**(12), 1311-1330.
- Brigham, E.O. (1988), *The Fast Fourier Transform and its Applications*, Englewood Cliffs, NJ: Prentice-Hall.
- Chen, J., Hui, M.C.H. and Xu, Y.L. (2007), "A comparative study of stationary and non-stationary wind models using field measurements", *Bound. - Lay. Meteorol.*, **122**, 105-121.
- Chen, J., Ma, J. and Wu, M. (2012), "Unified Non-stationary mathematical model for near-ground surface strong winds", *Proceedings of the World Congress on Advances in Civil, Environmental, and Materials Research (ACEM' 12)*, Seoul, Korea.
- Chen, L. and Letchford, C.W. (2004), "A deterministic-stochastic hybrid model of downbursts and its impact on a cantilevered structure", *Eng. Struct.*, **26**, 619-629.
- Das, N.K. (1988), "Safety analysis of steel building frame under dynamic load", Ph.D. Dissertation, Texas Tech University, Texas USA.
- Ellingwood, B.R., Galambos, T.V., MacGregor, J.G. and Cornell, C.A. (1980), Development of probability based load criterion for American National Standard A.58, NBS Special Publication 577, US Department of Commerce, Washington DC.
- Fang, K.T., Lu, X., Tang, Y. and Yin, J.X. (2004), 'Constructions of uniform designs by using resolvable packings and coverings', *Discrete Math.*, **274**, 25-40.
- FEMA 356 (2000), *Prestandard and commentary for the Seismic Rehabilitation of Buildings*, Federal Emergency Management Agency Washington, D.C.
- Ghosh, S., Mitra, S., Ghosh, S. and Chakraborty, S. (2016), "Seismic reliability analysis in the framework of metamodelling based Monte Carlo Simulation, modeling and simulation techniques in structural engineering", *IGI Global*, 192, August.
- Goswami, S., Ghosh, S. and Chakaraborty, S (2016), "Reliability Analysis of Structures by iterative improved response surface method", *Struct. Saf.*, **60**, 56-66.
- Gupta, S. and Manohar, C.S. (2004), "An improved response surface method for the determination of failure probability and importance measures", *Struct. Saf.*, **26**, 123-139.
- Gur, S. and Chaudhuri, S.R. (2014), "Vulnerability assessment of container cranes under stochastic wind loading", *Struct. Infrastruct. Eng.*, **12**, 1511-1530.
- Harris, R.I. (1990), "Some further thoughts on the spectrum of gustiness in strong winds", *J. Wind Eng. Ind. Aerod.*, **33**, 461-477.
- Hjelmfelt, M.R. (1988), "Structure and life circle of microburst outflows observed in Colorado", *J. Appl. Meteorol.*, **27**, 900-927.
- Holmes, J.D. and Oliver, S.E. (2000), "An empirical model of a downburst", *Eng. Struct.*, **22**, 1167-1172.
- IS: 456, (2000), *Plain and reinforced concrete - Code of practice*, Bureau of Indian Standards: India.
- IS: 875(Part 3)-2015 (2015), *Indian Standard Code of practice for design Loads (other than Earthquake) for Building and structures, Part 3: Wind Loads*, Bureau of Indian Standards: India.
- Kaimal, J.C., Wyngaard, J.C., Izumi, Y. and Cote, O.R. (1972), "Spectral Characteristics of surface layer turbulence", *J. Roy. Meteorol. Soc.*, **98**, 563-589.
- Kang, S., Koh, H. and Choo, J.F. (2010), "An efficient response surface Method using moving least squares approximations for structural reliability analysis", *Probab. Eng. Mech.*, **25**, 365-371.
- Kim, C., Choi, K.K. and Wang, S.(2005), "Efficient response surface modeling by using moving least-square method and sensitivity", *AIAA J.*, **43**(11), 2404-2411.
- Konthesingha, K.M.C., Stewart, M.G., Paraic, R., Ginger, J. and Henderson, D. (2015), "Reliability based vulnerability modelling of metal-clad industrial buildings to extreme wind loading for cyclonic regions", *J. Wind Eng. Ind. Aerod.*, **147**, 176-185.
- Kwon, D.K. and Kareem, A. (2009), "Gust-front factor: New framework for wind load effects on structures", *J. Struct. Eng.*, **135** (6), 717-732.
- Lu, Q., Xiao, Z., Ji, J., Zheng, J. and Shang, Y. (2017), "Moving least square method for reliability assessment of rock tunnel excavation considering ground-support interactions", *Comput. Geotech.*, **84**, 88-100.
- Mander, J.B. and Priestley, M.J.N. (1988), "Theoretical stress-strain model for confined concrete", *J. Struct. Eng.*, **114**(8), 1804-1826.
- Marra, A.S. and Luca, C. (2011), "A Monte Carlo based method for the dynamic fragility analysis of tall buildings under turbulent wind loading", *Eng. Struct.*, **33**, 410-420.
- MATLAB, The MathWorks, Inc., Natick, Massachusetts, United States.
- Morgan, E.C., Matthew, L., Vogel, R.M. and Laurie, G.B. (2011), "Probability distributions for offshore wind speeds", *Energ. Convers. Manage.*, **52**, 15-26.
- Myers, R.H. and Montgomery, D.C. (1995), *Response Surface Methodology: Process and Product in Optimization Using Designed Experiments*, John Wiley & Sons, Inc. New York, NY, USA.
- Peng, Y., Wang, Z. and Ai, X. (2018), "Wind-induced fragility assessment of urban trees with structural uncertainties", *Wind Struct.*, **26**(1), 45-56.
- Popescu, R., Deodatis, G. and Prevost, J.H. (1998), "Simulation of homogeneous non-Gaussian stochastic vector fields", *Probab. Eng. Mech.*, **13**(1), 1-13.
- Repetto, M.P. and Solari, G. (2004), "Directional wind-induced fatigue of slender vertical structures", *J. Struct. Eng.*, **130**(7), 1032-1040.
- Sarkar, A., Gugliani, G. and Deep, S. (2017), "Weibull model for wind speed data analysis of different locations in India", *J. Civil Eng. - KSCE*, 1-13.
- Sarkar, A., Sindh, S. and Mitra, D. (2011), "Wind climate modelling using weibull and extreme value distribution", *Int. J. Eng. Sci. Technol.*, **3**(5), 100-106.
- Shinozuka, M. and Jan, C.M. (1972), "Digital Simulation of Random Processes and Its Applications," *Journal of Sound and Vibration*, **25**, 111-128.
- Simiu, E. and Scanlan, R.H. (1986), *Wind Effects on Structures: An Introduction to Wind Engineering*, John Wiley & Sons, Hoboken.
- Spagnoli, A. and Montanari, L. (2013), "Along-wind simplified analysis of wind turbines through a coupled blade-tower model", *Wind Struct.*, **17**(6), 589-607.
- Song, C.Y., Lee, J. and Choung, J.M. (2011), "Reliability-based design optimization of an FPSO riser support using moving least square response surface meta models", *Ocean Eng.*, **38**, 304-318.
- Spanos, P.T.D. (1980), "Numerical solutions of a van der pol oscillator", *Comput. Math. Appl.*, **6**(1), 135-145.
- SAP 2000NL, Computer and Structures, Inc. (CSI) (2009).
- Taflanidis, A.A. and Cheung, S.H. (2012), "Stochastic sampling using moving least squares response surface methodologies",

- Probab. Eng. Mech.*, **28**, 216- 224.
- Taflanidis, A.A., Jia, G. and Gidaris, I. (2016), “Natural hazard probabilistic risk assessment through surrogate modeling”, *Multi-hazard Approaches to Civil Infrastructure Engineering*, Springer International Publishing, 59-86.
- Venanzi, I., Materazzi, A.L. and Ierimonti, L. (2015), “Robust and reliable optimization of wind-excited cable-stayed masts”, *J. Wind Eng. Ind. Aerod.*, **147**, 368-379.
- Zhang, L., Lia, J. and Peng, Y.P. (2008), “Dynamic response and reliability analysis of tall buildings subject to wind loading”, *J. Wind Eng. Ind. Aerod.*, **96**(1), 25-40.

CC